C.P. No. 325
(17,833)
A.R.C. Technical Report

C.P. No. 325
(17,833)
A.R.C. Technical Report

MINISTRY OF SUPPLY

AERONAUTICAL RESEARCH COUNCIL

CURRENT PAPERS

The Influence of Design Pressure Ratio and Divergence Angle on the Thrust of Convergent-Divergent Propelling Nozzles

By

P. F. Ashwood, and D. G. Higgins

LONDON HER MAJESTY'S STATIONERY OFFICE

1957

FIVE SHILLINGS NET

C.P. No. 325

Report No. R.168

January, 1955.

NATIONAL GAS TURBINE ESTABLISHMENT

The influence of design pressure ratio and divergence angle on the thrust of convergent-divergent propelling nozzles

- by -

P. F. Ashwood and D. G. Higgins

SUMMARY

Tests have been made to determine the thrusts obtainable from two groups of Laval-type convergent-divergent propelling nozzles over a range of pressure ratios up to 9 : 1 using air at sensibly ambient temperature. The nozzles of the first group were designed for pressure ratios of 4, 6, 8, 10 and 12 and had an included divergence angle of 20° whilst those of the second group were all designed for a pressure ratio of 8 and had included divergence angles of 5°, 10°, 20°, 30° and 50°.

The superior thrust performance at high pressure ratios of the Laval-type nozzles over that of a plain convergent nozzle has been demonstrated. The effect of divergence angle on the thrust has been examined and, within the range 5° to 25°, been found to be small.

A comparison between the performance of a Busemann-type profiled nozzle designed to give parallel flow at outlet and an equivalent nozzle having a straight conical divergence has shown that at the design point the profiled nozzle gives about 2 per cent more thrust.

All the nozzles tested, with the exception of one having 5° divergence angle, exhibited a form of jet instability at very low pressure ratios. The conditions under which this occurs are presented graphically.

CONTENTS

		Page
1.0	Introduction	4
2.0	Test apparatus	4
2.1	Model nozzles	4
2.2	Thrust balance	5
2.3	Pressure and temperature measurement	5
2.4	Air flow measurement	5
3.0	Experimental procedure	5
4.0	Theoretical performance of nozzles	6
4.1	Performance at design pressure ratio	6
4.2	Performance at off-design pressure ratio	6
5.0	Experimental results	7
5.1	Performance of Group I nozzles	7
5.2	Performance of Group II nozzles	9
5.3	Comparative performance of profiled and straight-taper nozzles	9
5.4	Jet instability	9
6.0	Conclusions	10
Acknowledgment		10
List of symbols		11
References		12

TABLES

No.	Title	
I	Design details of model nozzles	5
II	"Kink" points for Group I nozzles	8
Appendix I		13

ILLUSTRATIONS

Fig. No.	Title
1	Model nozzles
2	Profiled and equivalent conical nozzles

ILLUSTRATIONS (cont'd)

Fig. No.	Title
3	General arrangement of thrust rig
4	Variation of non-dimensional thrust with pressure ratio for Group I nezzles
5	Magnified section of Figure 4
6	Variation of specific thrust with pressure ratio for Group I nozzles
7	Magnified section of Figure 6
8	Variation of C_F and C_T with pressure ratio for Group I nozzles
9	Variation of non-dimensional thrust with pressure ratio for Group II nozzles
10	Variation of specific thrust with pressure ratio for Group II nozzles
11	Variation of C_F and C_T with pressure ratio for Group II nozzles
12	Variation of non-dimensional thrust with included divergence angle for Group II nozzles
13	Variation of non-dimensional thrust with pressure ratio for profiled nozzle and equivalent nozzle with plain conical divergence
14	Variation of specific thrust with pressure ratio for profiled nozzle and equivalent nozzle with plain conical divergence
15	Variation of Δ with design pressure ratio E
16	Diagram showing regions of jet instability

1.0 Introduction

The work described in this Report is an extension of an earlier investigation which has been previously reported (Reference 1) and was undertaken primarily in order to investigate the performance of Lavel-type convergent-divergent nozzles at off-design conditions. In particular, information was required on the effect of divergence angle on the thrust and the benefits to be obtained by the use of a profiled divergent portion designed to give parallel flow at exit.

2.0 Test apparatus

2.1 Model nozzles

Altogether eleven convergent-divergent nozzles were tested. They were divided into two main groups, the first group having constant divergence angle and varying design pressure ratio * and the second group having constant design pressure ratio and varying divergence angle. The nozzles of Group I had an included angle of divergence of 20° and were designed for pressure ratios of 4, 6, 8, 10 and 12, whilst those of Group II had a constant design pressure ratio of 8 and divergence angles of 5, 10, 30 and 50°. All the nozzles in these two groups were geometrically similar, the inlet profile being circular and the divergent portion conical.

For the investigation into the effect of divergent section profile, a nozzle designed to give an exit Mach Number of 2 was used. The co-ordinates for the supersonic portion of this nozzle were obtained using a method originated by R. Sargent, this being a development of the classical method of characteristics with empirical boundary layer corrections. A cubic curve was used to define the approach section. For comparison, a Laval-type nozzle with conical divergence having the same inlet profile and design pressure ratio was also tested.

In addition to the nozzles described above a conical convergent nozzle of 25° included angle was tested.

The nozzles were made of brass and were given a high internal polish. The nominal throat diameters were 1 in. but these were checked individually by inserting a slightly tapered mandrel coated with marking blue into the bore and measuring its diameter at the point where the blue was removed by contact with the throat. It was considered that in this way the throat diameter could be determined to within ±0.0025 in. The outlet diameters were measured with a travelling microscope and were considered accurate to within ±0.0005 in.

Comparative drawings of the model nozzles are shown in Figures 1 and 2 and their principal design features are given in Table I (see over).

---

* Throughout this Report the term "design pressure ratio" refers to that value which corresponds with the given area ratio assuming one-dimensional isentropic flow.

TABLE I

Design details of model nozzles

Nominal Pressure Ratio	Divergence Angle	Throat dia.	Exit dia.	Area Ratio	Design Pressure Ratio	Design Exit Mach No.	Remarks
4	20	1.0030	1.110	1.225	4.05	1.568	Group I
6	20	1.0025	1.218	1.476	6.04	1.833	
8	20	1.0037	1.320	1.730	8.20	2.032	
10	20	1.0012	1.395	1.941	10.08	2.165	
12	20	1.0028	1.464	2.131	11.92	2.265	
8	50	0.9993	1.312	1.724	8.15	2.025	Group II
8	30	1.0012	1.320	1.738	8.28	2.035	
8	10	1.0016	1.320	1.737	8.26	2.033	
8	5	1.0045	1.320	1.727	8.18	2.029	
-	-	1.002	1.313	1.717	7.83	2.000	Profiled nozzle
-	8° 52'	0.999	1.3225	1.752	8.39	2.046	Equivalent plain conical nozzle

2.2 Thrust balance

Throughout the present investigation thrust was measured using the strain gauge apparatus described in Reference 2. With this it was possible to measure a maximum thrust of 150 lb. to an accuracy of ±0.1 lb. with an internal pressure in the supply pipe of 10 atmospheres. The rig is illustrated in Figure 3.

2.3 Pressure and temperature measurement

To establish the inlet conditions the total pressure and temperature were measured in the air supply pipe immediately before the nozzle. Since the velocity in the supply pipe was very low, the Mach number never exceeding 0.06, it was considered sufficiently accurate to use single point measurements. The total pressure was therefore determined from one centrally mounted pitot tube and the temperature with a mercury-in-glass thermometer.

2.4 Airflow measurement

An orifice plate made and installed according to the standards laid down in B.S.1042 was used to measure the air flow.

3.0 Experimental procedure

Each nozzle was tested over a range of pressure ratios up to the maximum obtainable, that is slightly over 9 : 1. Measurements of thrust,

inlet total pressure, inlet temperature and air mass flow were made for each condition. The thrust balance was calibrated at frequent intervals both at atmospheric pressure and with the nozzle sealed and the pipe pressurized to 9 atmospheres. At all times the calibrations were consistent to within ±0.1 lb., and no hysteresis between increasing and decreasing pressure was observed. It was, however, found necessary to connect the electrical supply to the strain gauge circuit about 30 minutes before testing commenced in order to allow the resistive components of the circuit to attain an equilibrium temperature. For the last 5 minutes of this time the air supply to the rig was turned on. This was found to be essential, because the supply air temperature was usually 5 to 10°C. above ambient in the test cubicle, and whilst the overall temperature level in no way affected the thrust balance calibration, any temperature difference between the two strain gauges produced errors of the order of 0.2 lb. indicated thrust/°C. temperature difference.

4.0 Theoretical performance of nozzles

4.1 Performance at design pressure ratio

A simple analysis, based on one-dimensional isentropic flow, of the variation of thrust with design pressure ratio is given in the Appendix. It is there shown that the non-dimensional thrust assuming complete expansion to atmospheric pressure is given by:

$$\frac{F}{A_2 P_{1_t}} = \frac{K^2 R}{g} \frac{A_2}{A_3} \left(\frac{P_{1_t}}{P_a} \right)^{\frac{1}{\gamma}} \qquad \ldots\ldots\ldots\ldots (1)$$

which for air with $\gamma = 1.4$ becomes:-

$$\frac{F}{A_2 P_{1_t}} = 0.4689 \frac{A_2}{A_3} \left(\frac{P_{1_t}}{P_a} \right)^{0.7143} \qquad \ldots\ldots\ldots\ldots (2)$$

For a convergent nozzle operating above the choking pressure ratio

$$\frac{F}{A_2 P_{1_t}} = \frac{K^2 R}{g} \cdot \left(\frac{P_{1_t}}{P_{3_s}} \right)^{\frac{1}{\gamma}} + \frac{P_{3_s}}{P_{1_t}} - \frac{P_a}{P_{1_t}} \qquad \ldots\ldots\ldots (3)$$

which for air is:-

$$\frac{F}{A_2 P_{1_t}} = 1.268 - \frac{P_a}{P_{1_t}} \qquad \ldots\ldots\ldots\ldots\ldots\ldots (4)$$

4.2 Performance at off-design pressure ratio

Away from the design point, Equation (1) requires to be modified by the addition of a pressure thrust term, as shown in the Appendix. Thus the non-dimensional thrust is:-

$$\frac{F}{A_2 P_{1_t}} = \frac{K^2 R}{g} \cdot \frac{A_2}{A_3} \left(\frac{P_{1_t}}{P_{3_s}} \right)^{\frac{1}{\gamma}} + \left(\frac{P_{3_s}}{P_{1_t}} - \frac{P_a}{P_{1_t}} \right) \frac{A_3}{A_2} \quad .. (5)$$

Classic one-dimensional theory assumes that the shock system moves inside the nozzle when the overall pressure ratio is reduced below that value which enables a normal shock located exactly at the exit plane to restore the pressure to ambient. An expression for this limiting condition is derived in the Appendix and it is shown that if a normal shock is assumed the lowest overall pressure ratio at which a nozzle can run full is given by:-

$$\left(\frac{P_{1_t}}{P_a} \right)_{\text{limit}} = \frac{\left\{ 1 + \frac{\gamma - 1}{2} M_3^2 \right\}^{\frac{\gamma}{\gamma - 1}}}{\left\{ \frac{2\gamma}{\gamma + 1} M_3^2 - \frac{\gamma - 1}{\gamma + 1} \right\}} \quad .. .. (6)$$

where M_3 = design exit Mach number

given by $$M_3^2 = \frac{2}{\gamma - 1} \left\{ \left(\frac{P_{1_t}}{P_{3_s}} \right)^{\frac{\gamma - 1}{\gamma}} - 1 \right\} \quad .. .. .. (7)$$

5.0 Experimental results

5.1 Performance of Group I nozzles

The results of the tests on the nozzles of Group I are shown in terms of non-dimensional thrust in Figures 4 and 5 and in terms of specific thrust in Figures 6 and 7. From these graphs it will be seen that for conditions under which complete expansion occurs within the nozzle, linear relationships exist between $F/A_2P_{1_t}$ and Pa/P_{1_t} and between $F/W\sqrt{T_{1_t}}$ and Pa/P_{1_t}. This is as predicted by the one-dimensional analysis. The results for the convergent nozzle are also plotted in Figures 4, 5, 6 and 7 for comparison.

In Figure 8 the results are expressed in terms of thrust coefficients. These are defined as the ratios of the measured non-dimensional and specific thrusts to values calculated assuming complete isentropic expansion to ambient pressure. It can readily be shown that the ratio C_F/C_T is the discharge coefficient of the nozzle.

It will be seen from Figure 8 that the thrust coefficients attain maximum values at approximately the design pressure ratio, the maxima exhibiting a tendency to increase with design pressure ratio. This is contrary to expectation since it is logical to suppose that for nozzles of constant divergence angle frictional losses will increase with design pressure ratio.

It is possible that it may be a Reynolds number effect since with the method of testing used the value of Re at the throat increases roughly in proportion to the applied pressure ratio.

The range of Re (based on throat diameter) covered by the model tests extended from about 3×10^5 to 3.5×10^6. In a typical engine having a maximum gas temperature of 1200°K., values of Re (based on a 1 ft. diameter nozzle) would vary from 7.5×10^5 at M = 3, 75,000 ft. to 1.1×10^6 at M = 1.2, 40,000 ft. The corresponding value at take off conditions would be 2.2×10^6.

Inspection of Figure 4 shows that the non-dimensional thrust varies linearly with Pa/P_{1_t} both above and below the design pressure ratio. This is as predicted by Equation (5), the constant of proportionality being the area ratio A_3/A_2. The highest value of Pa/P_{1_t} to which the proportionality extends has been termed the "kink" point and this represents the limiting condition at which the nozzle runs full. Any further increase of Pa/P_{1_t} beyond the kink point value causes the shock to move inside the nozzle with the result that the area on which the pressure thrust acts is reduced. Values of kink point for the Group I nozzles are given in Table II below.

TABLE II

Kink points for Group I nozzles

Design Pressure Ratio E	$(P_a/P_{1_t})_{kink}$	$\Delta = \frac{(P_{1_t}/P_a)_{kink}}{E}$
4.05	0.432	0.572
6.04	0.330	0.502
8.20	0.273	0.447
10.08	0.248	0.400
11.92	0.234	0.358

These results are shown plotted in Figure 15. This shows that the nozzle ceases to run full at an applied pressure ratio appreciably higher than that predicted by the simple theory of Section 4.2. This is due to shock wave-boundary layer interaction for as the applied pressure ratio is reduced the pressure ratio across the exit shock increases until a value is reached which the boundary layer is unable to support. The result is that detachment of the flow then occurs and the shock waves become re-established at a new position within the nozzle. The conditions under which this occurs have been more fully explored in Reference 3.

In the present tests the simplest empirical expression which best fits the experimental points is $\Delta = 1/E^{0.396}$. It is, however, recommended

that this formula should be applied with reserve and be treated as a guide only. This is because determinations of the kink points from the thrust measurements are not considered to be of great accuracy. A more satisfactory technique is to measure the axial pressure distribution near the nozzle exit (Reference 3) or alternatively to visualize the shock pattern by means of shadowgraphs.

5.2 Performance of Group II nozzles

The variations of non-dimensional and specific thrust with P_a/P_{1_t} for the Group II nozzles are shown in Figures 9 and 10 and the corresponding thrust coefficients in Figure 11. The curves are in general similar in form to those for the Group I nozzles although a marked discontinuity is evident in the case of the 50° nozzle and this results in it having a performance at low pressure ratios similar to that given by the convergent nozzle. It is likely that this is due to the complete detachment of the flow in the diverging portion when operating away from the design condition.

Figure 12 shows a cross-plot of the results given in Figure 9 to illustrate the effect of divergence angle on the non-dimensional thrust. At the design pressure ratio (8 : 1) it is evident that the optimum divergence angle is about 11°, but the curve is quite flat and the angle can be varied between about 5° and 25° without reducing the thrust by more than 1 per cent below the maximum value.

5.3 Comparative performance of profiled and straight-taper nozzles

A comparison is given in Figures 13 and 14 between the non-dimensional and specific thrusts of the profiled and straight-taper nozzles illustrated in Figure 2. The results show that down to a pressure ratio of about 2.8, that is to about 35 per cent of the design value, the profiled nozzle gives the greater thrust. At its design pressure ratio of 7.83 the profiled nozzle gives approximately 2 per cent more thrust than does the equivalent conical nozzle.

The kink in the non-dimensional thrust curve occurs at a lower pressure ratio for the profiled nozzle than for the straight-taper one, the values of Δ being 0.325 and 0.378 respectively.

5.4 Jet instability

With the exception of the one having a 5° included divergence angle, all the convergent-divergent nozzles showed the same form of instability as that described in Reference 1. At low overall pressure ratios the flow detached from one side of the diverging section, the jet emerging at an angle to the main axis of the nozzle. The circumferential position at which detachment occurred changed with time in a completely random manner, the flow on some occasions remaining steady for several seconds and then changing position several times in rapid succession. The effect is thought to be the same as that observed in wide angle subsonic diffusers, the random change of direction being due to local disturbances in the flow "triggering" the deflection.

The conditions under which instability was observed with the Group I nozzles are indicated in Figure 16.

On this graph the full line indicates the limiting condition at which sonic velocity is just reached in the throat and the two dotted lines the limits of instability. At any point above the upper dotted line the jet was observed to be definitely stable and conversely for the region below the lower dotted line. In the region between the dotted lines the nature of the flow was indeterminate, instability occurring only occasionally.

Two conclusions can be drawn from Figure 16:-

(1) Instability does not occur in nozzles designed for pressure ratios less than 4.

(2) On any nozzle instability will not occur as long as the overall pressure ratio exceeds 2.2.

6.0 Conclusions

The following conclusions were drawn from the tests:-

(1) At pressure ratios above 4.85 the thrust from all the Laval-type nozzles was greater than that from the convergent nozzle. Each individual nozzle was superior to the convergent nozzle at all pressure ratios greater than about half its design value.

(2) For each nozzle, the non-dimensional and specific thrust coefficients attained maximum values at approximately the design pressure ratio. In the case of the nozzles having constant divergence angle the maxima showed a tendency to increase with design pressure ratio, an effect contrary to expectation.

(3) So far as thrust was concerned, the best included divergence angle was found to be about 12° although within the range 5° to 25° the divergence angle affected the thrust by less than 1 per cent.

(4) A profiled nozzle designed to give parallel flow at exit gave a greater thrust than an equivalent nozzle having a plain conical divergence at all pressure ratios greater than about 0.35 of the design value.

(5) At overall pressure ratios less than 2.2 all the nozzles having an included divergence angle greater than 5° exhibited an instability wherein the flow detached from one side of the divergent section. This caused the jet to emerge at an angle to the main axis of the nozzle and changed the line of action of the thrust. The position of detachment and the time interval between changes varied in a completely random manner.

ACKNOWLEDGMENT

The authors wish to record their indebtedness to Mr. P. J. Fletcher who was responsible for a large part of the experimental work described in this Report.

SYMBOLS

Symbol	Quantity	Units
A	Area	sq.in.
C_F	Non-dimensional thrust coefficient	
C_T	Specific thrust coefficient	
Δ	$\frac{\text{Limiting applied pressure ratio for shock at nozzle exit}}{\text{Design pressure ratio}}$	
E	Design pressure ratio	
F	Gross thrust	lb.
g	Gravitational constant (taken as 32.2 ft./sec./sec.)	ft./sec./sec.
γ	Ratio of specific heats	
K	Non-dimensional mass flow*	
M	Mach number	
P	Pressure	lb./sq.in.abs.
R	Gas constant (taken as 96.0 ft lb./lb./°C.)	ft.lb./lb./°C.
T	Temperature	°K.
W	Air mass flow	lb./sec.

Suffices

1	Nozzle inlet
2	Nozzle throat
3	Nozzle exit
a	Ambient
t	Total conditions
s	Static conditions

---

* This is defined as $\frac{W\sqrt{T_{1_t}}}{A_2 P_{1_t}}$. For air $\gamma = 1.4$ so that using the units quoted above the value of non-dimensional flow corresponding to unity Mach number is 0.3966.

REFERENCES

No.	Author	Title
1	P. J. Fletcher	Measurements of thrust from convergent-divergent propelling nozzles. N.G.T.E. Memorandum No. M.144. A.R.C. 14,739. February, 1952.
2	P. J. Fletcher	A method for measuring the reaction force of a high pressure gas stream. N.G.T.E. Memorandum No. M.184. March, 1953.
3	G. W. Crosse and P. F. Ashwood	The influence of pressure ratio and divergence angle on the shock position in two-dimensional, over-expanded, Laval-type, convergent-divergent nozzles. (Unpublished).

APPENDIX I

(i) Performance of an ideal nozzle at its design pressure ratio

$$\text{Gross thrust } F = \frac{WV_3}{g}$$

$$= \frac{W^2 . R\, T_{3_s}}{g\, A_3\, P_{3_s}}$$

$$= \frac{K^2\, A_2^2\, P_{1_t}^2\, R\, T_{3_s}}{P_{1_t}\, g\, A_3\, P_{3_s}} \qquad \ldots\ldots\ldots\ldots\ldots\ldots (a)$$

$\therefore$ Non-dimensional thrust

$$\frac{F}{A_2 P_{1_t}} = \frac{K^2 R}{g} \cdot \frac{A_2}{A_3} \cdot \frac{P_{1_t}}{P_{3_s}} \cdot \frac{T_{3_s}}{T_{1_t}}$$

$$= \frac{K^2 R}{g} \cdot \frac{A_2}{A_3} \left(\frac{P_{1_t}}{P_{3_s}}\right)^{\frac{1}{\gamma}} \qquad \ldots\ldots\ldots\ldots\ldots\ldots (b)$$

and specific thrust

$$\frac{F}{W\sqrt{T_{1_t}}} = \frac{K R}{g} \cdot \frac{A_2}{A_3} \cdot \frac{T_{3_s}}{T_{1_t}} \cdot \frac{P_{1_t}}{P_{3_s}}$$

(ii) Performance of an ideal nozzle at off-design conditions

Away from the design point, the exit static pressure differs from ambient and there is a pressure thrust term to be taken into account. This has, therefore, to be added to Equation (a) above. Thus:-

$$\text{Pressure thrust} = (P_{3_s} - P_a)\, A_3$$

and the non-dimensional thrust thus becomes:-

$$\frac{F}{A_2 P_{1_t}} = \frac{K^2 R}{g} \cdot \frac{A_2}{A_3} \left(\frac{P_{1_t}}{P_{3_s}}\right)^{\frac{1}{\gamma}} + \frac{P_{3_s}}{P_{1_t}} \cdot \frac{A_3}{A_2} - \frac{P_a}{P_{1_t}} \cdot \frac{A_3}{A_2} \qquad \ldots (c)$$

and the specific thrust

$$\frac{F}{W\sqrt{T_{1_t}}} = \frac{K\,R}{g} \cdot \frac{A_2}{A_3} \cdot \frac{T_{3_s}}{T_{1_t}} \cdot \frac{P_{1_t}}{P_{3_s}} + \frac{A_3\,P_{3_s}}{KA_2P_{1_t}} - \frac{{}'_3\,F_e}{KA_2P_{1_t}}$$

When the nozzle is under-expanded, that is, when the applied pressure ratio is greater than the design value, the pressure thrust term is positive. When the nozzle is over-expanded, $P_{3_s} < P_a$ and the pressure thrust term becomes negative. As the applied pressure ratio is reduced the discrepancy between the exit static pressure and ambient increases. The strength of the shock system downstream of the nozzle therefore increases until a limiting condition is reached when a normal shock exists exactly at the exit plane. Any further reduction of the overall pressure ratio across the nozzle causes this normal shock to move inside the nozzle.

Now the static pressure ratio across a normal shock is given by:-

$$r \equiv \frac{2\gamma}{\gamma+1}M^2 - \frac{\gamma-1}{\gamma+1}$$

$$= \frac{4\gamma}{(\gamma+1)(\gamma-1)}\left\{\left(\frac{P_{1_t}}{P_{3_s}}\right)^{\frac{\gamma-1}{\gamma}} - 1\right\} - \frac{\gamma-1}{\gamma+1}$$

Hence the limiting pressure ratio is:-

$$\left(\frac{P_{1_t}}{Pa}\right)_{limit} = \frac{P_{1_t}}{P_{3_s}} \cdot \frac{1}{r}$$

$$= \frac{P_{1_t}/P_{3_s}}{\frac{4\gamma}{(\gamma+1)(\gamma-1)}\left\{\left(\frac{P_{1_t}}{P_{3_s}}\right)^{\frac{\gamma-1}{\gamma}} - 1\right\} - \frac{\gamma-1}{\gamma+1}}$$

$$\therefore \Delta = \frac{\left(P_{1_t}/Pa\right)_{limit}}{P_{1_t}/P_{3_s}} = \frac{(\gamma+1)(\gamma-1)}{4\gamma\left(\frac{P_{1_t}}{P_{3_s}}\right)^{\frac{\gamma-1}{\gamma}} - (\gamma+1)^2} \quad \ldots\ldots\ldots\ldots (d)$$

With $\gamma = 1.4$ and for the range $4 < \left(\frac{P_{1_t}}{P_{3_s}}\right) < 12$ Equation (d) can be expressed to within $\pm\frac{1}{2}$ per cent as:-

$$\Delta = \frac{1}{\left(\frac{P_{1_t}}{P_{3_s}}\right)^{0.71}}$$

FIG. 1.

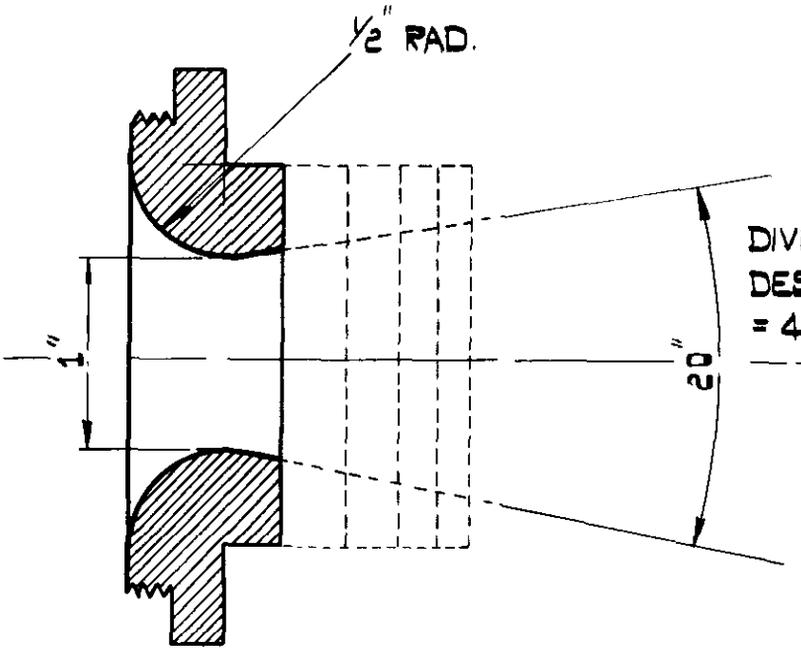

GROUP I

DIVERGENCE ANGLE = 20°

DESIGN PRESSURE RATIOS = 4·0, 6·0, 8·0, 10·0, & 12·0

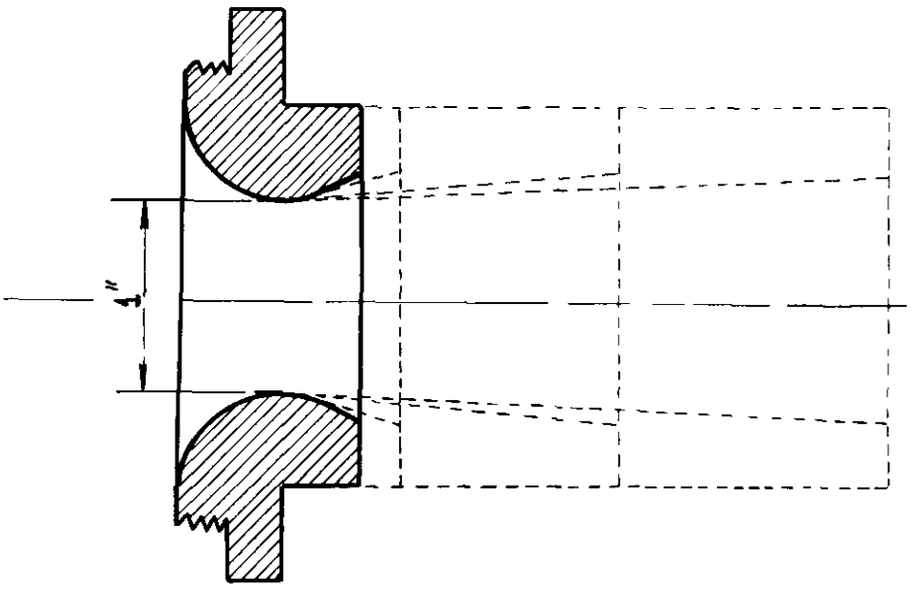

GROUP II

DESIGN PRESSURE RATIO = 8·0

DIVERGENCE ANGLES = 5°, 10°, 30°, & 50°.

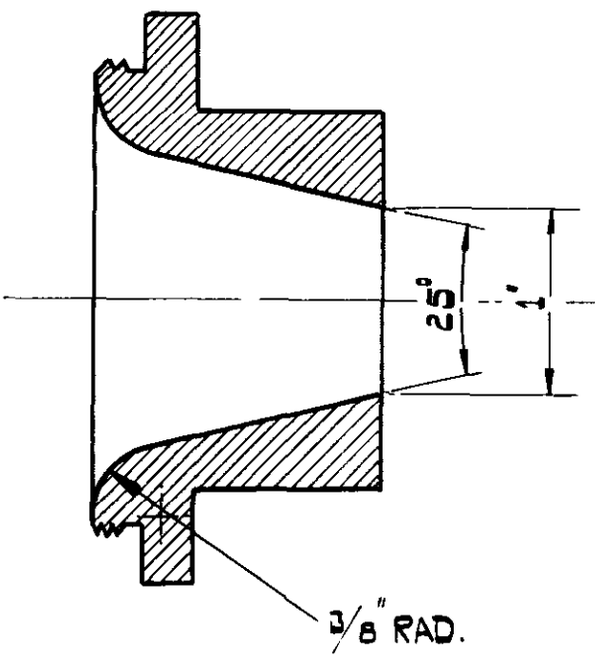

CONVERGENT NOZZLE.

CONVERGENCE ANGLE = 25°

MODEL NOZZLES

SK 58656

FIG. 2.

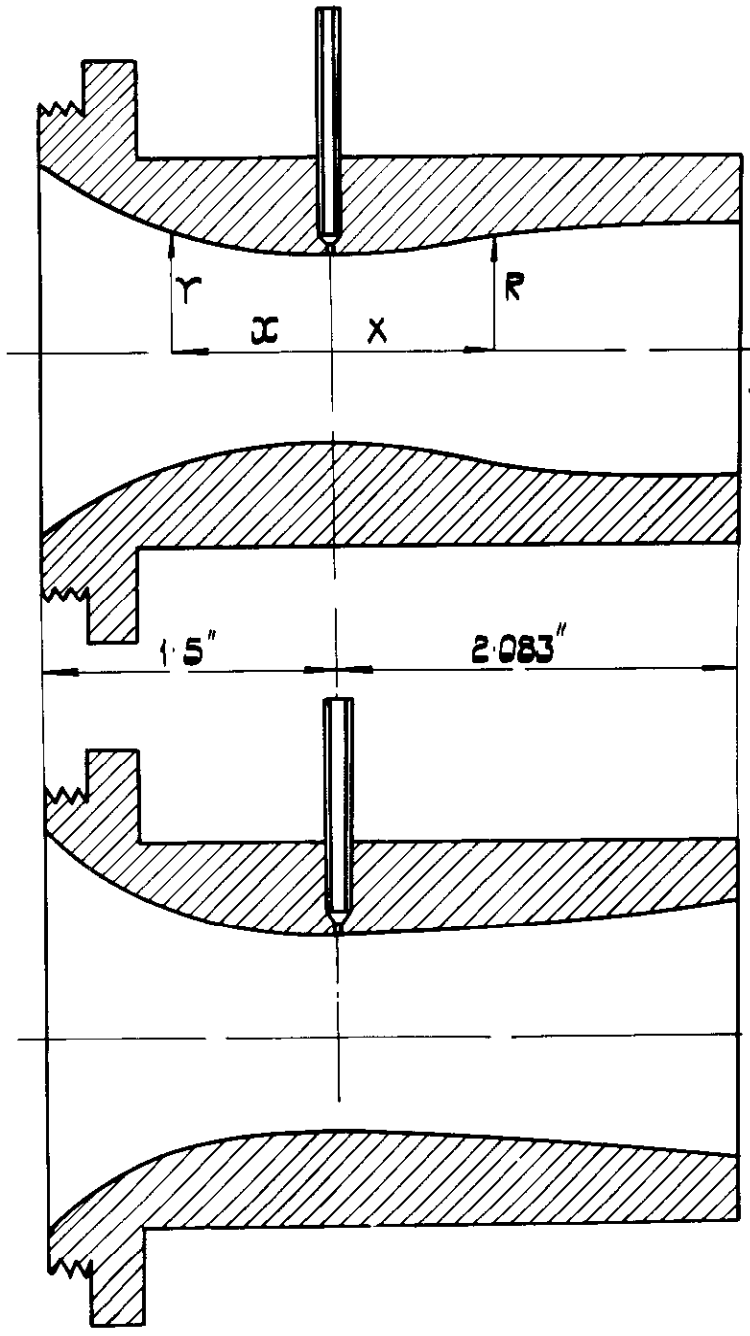

PROFILED NOZZLE

EQUIVALENT CONICAL DIVERGENCE NOZZLE.

INLET (SAME FOR BOTH NOZZLES)

x INS.	Y INS.
0·000	0·500
0·100	0·502
0·200	0·506
0·300	0·514
0·400	0·526
0·500	0·542
0·600	0·563
0·700	0·589
0·800	0·618
0·900	0·655
1·000	0·696
1·100	0·745
1·200	0·800
1·300	0·859
1·400	0·925
1·500	0·999

DIVERGENT PORTION FOR PROFILED NOZZLE

X INS	R INS
0·000	0·500
0·125	0·503
0·250	0·512
0·375	0·528
0·500	0·544
0·625	0·561
0·750	0·577
0·875	0·590
1·000	0·605
1·125	0·616
1·250	0·625
1·375	0·635
1·500	0·641
1·625	0·646
1·750	0·650
1·875	0·653
2·000	0·655
2·083	0·656

DIVERGENT PORTION FOR EQUIVALENT NOZZLE IS OF PLAIN CONICAL FORM WITH ORDINATES AS FOLLOWS :—

X = 0·10, R = 0·502.

X = 2·083, R = 0·656.

SK58657

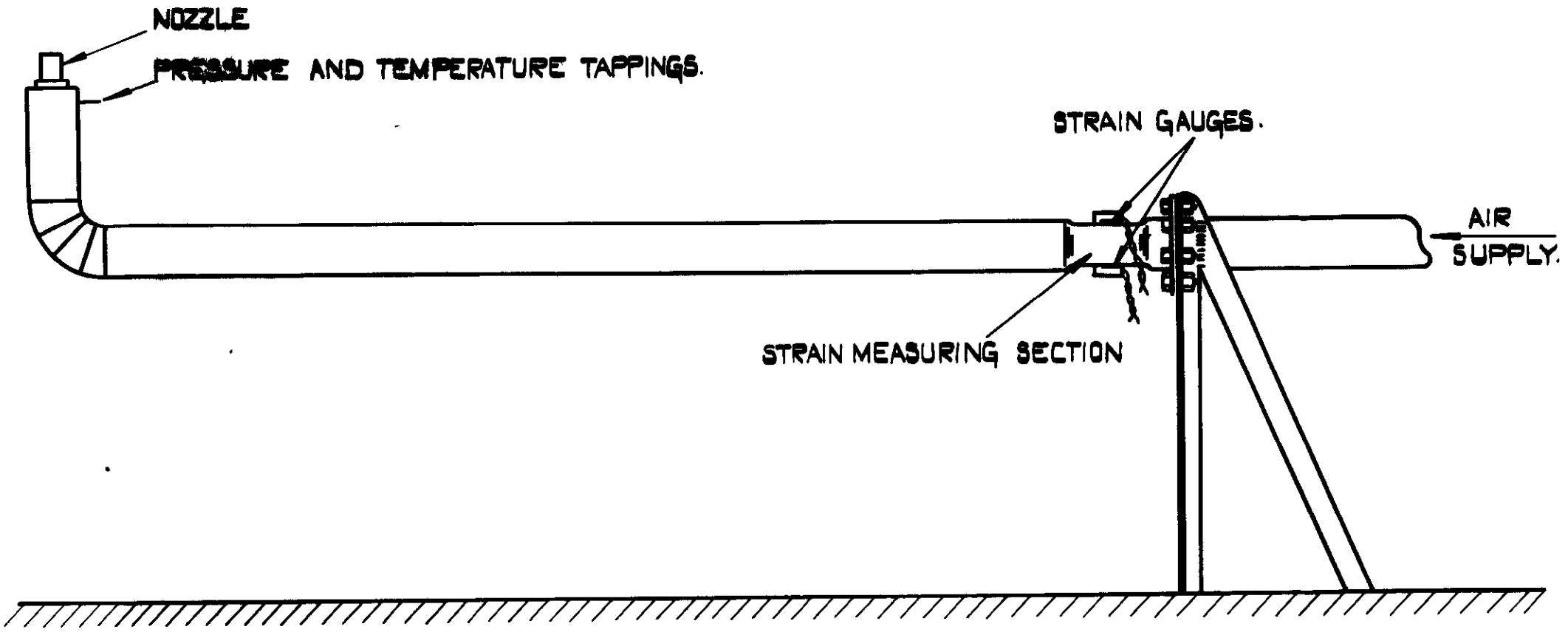

GENERAL ARRANGEMENT OF THRUST RIG.

FIG. 3

FIG. 4.

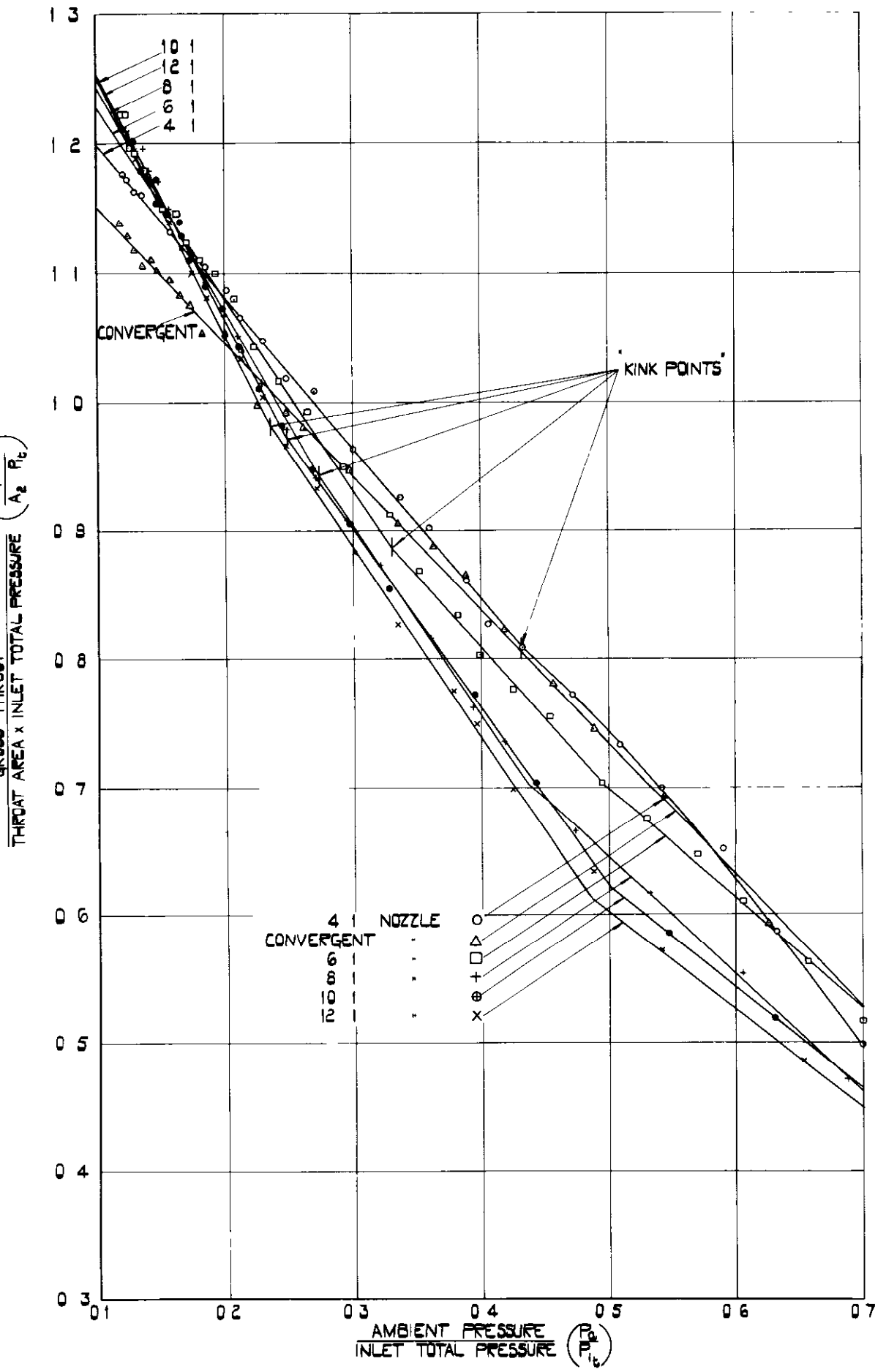

VARIATION OF NON-DIMENSIONAL THRUST WITH PRESSURE RATIO FOR GROUP I NOZZLES.

SK 50658

FIG. 5.

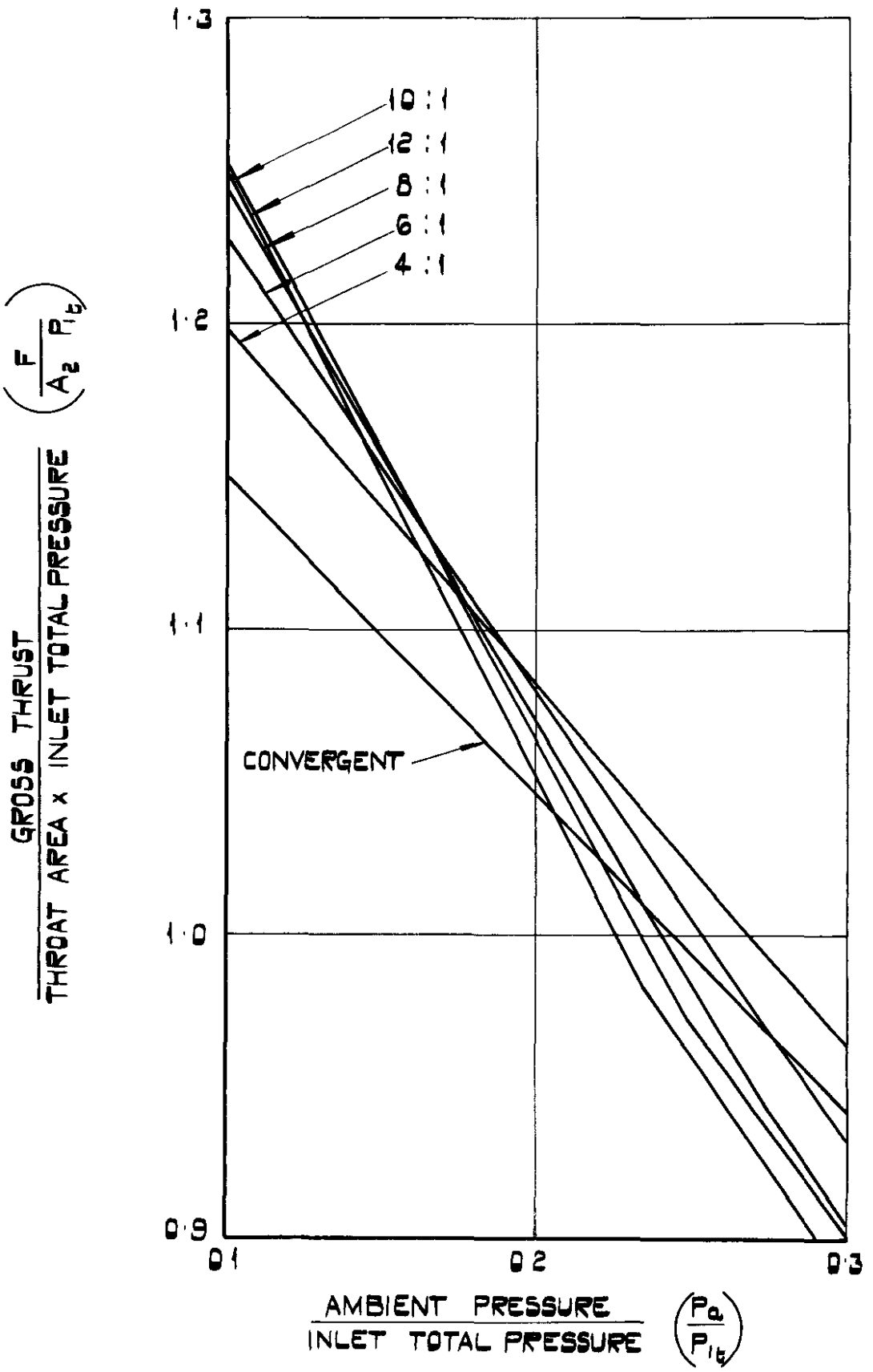

MAGNIFIED SECTION OF FIG. 4.

FIG. 6.

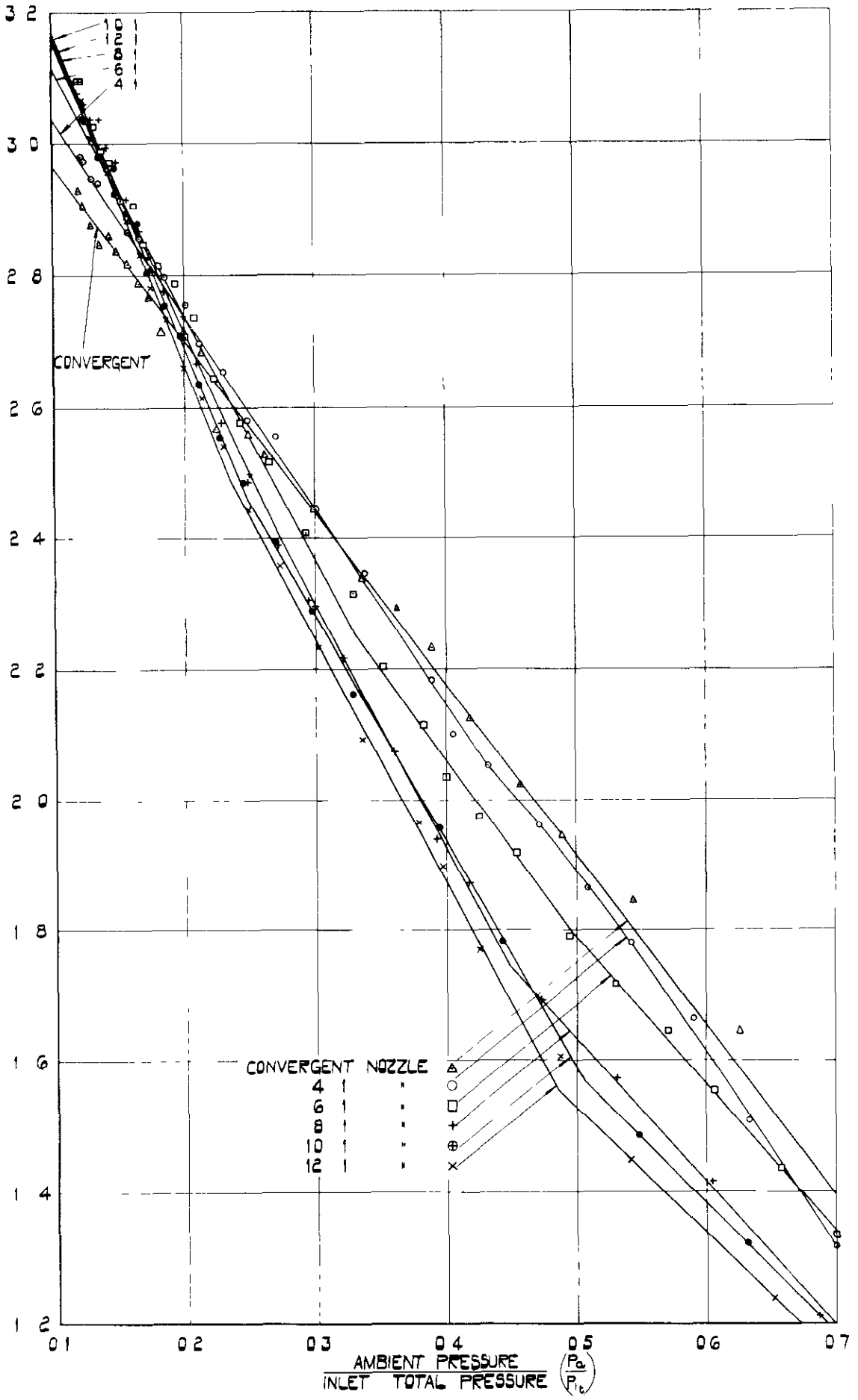

VARIATION OF SPECIFIC THRUST WITH PRESSURE RATIO FOR GROUP I NOZZLES.

SK 60021

SK 601 67

FIG. 7.

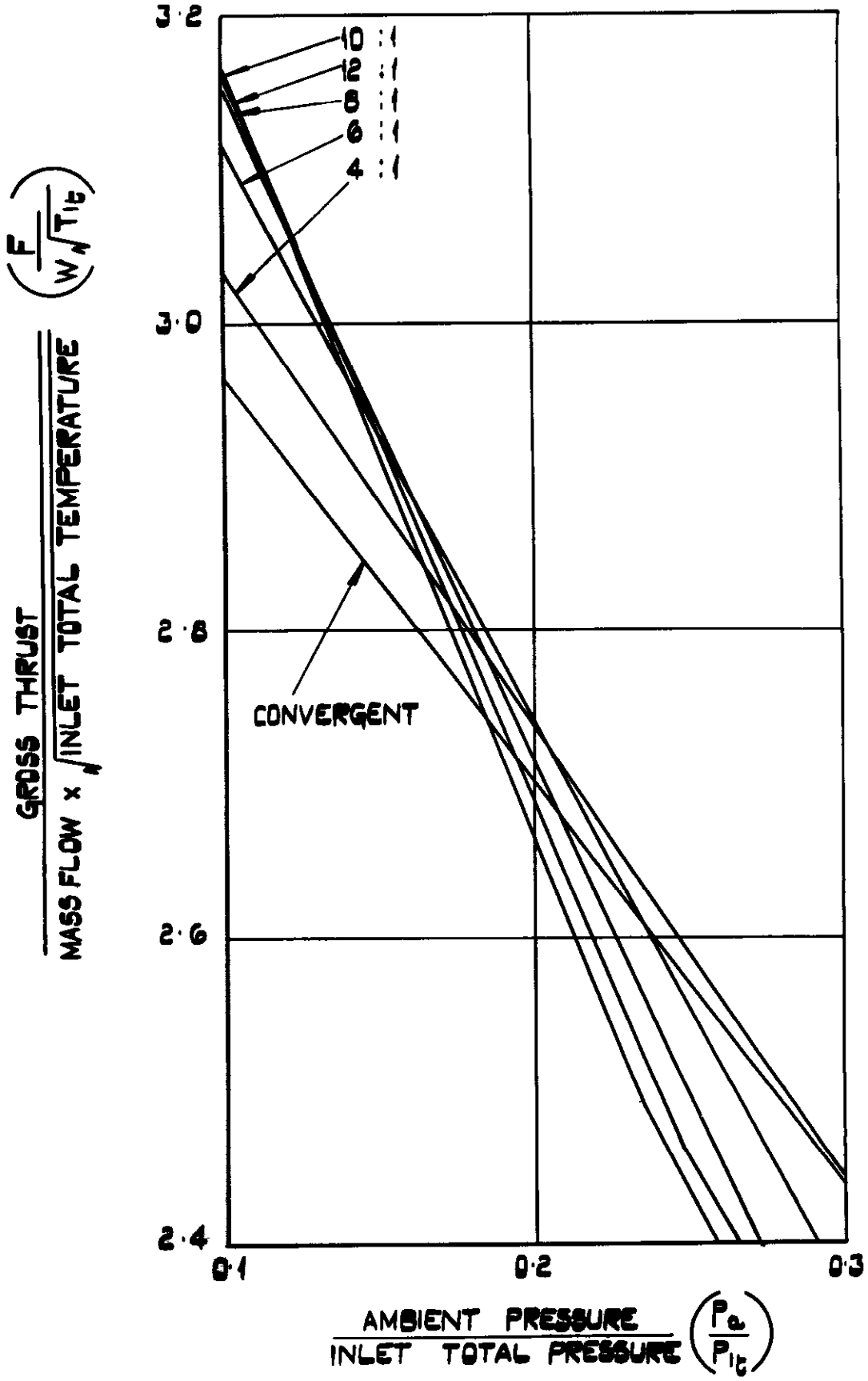

MAGNIFIED SECTION OF FIG. 6.

FIG. 8.

SK58660

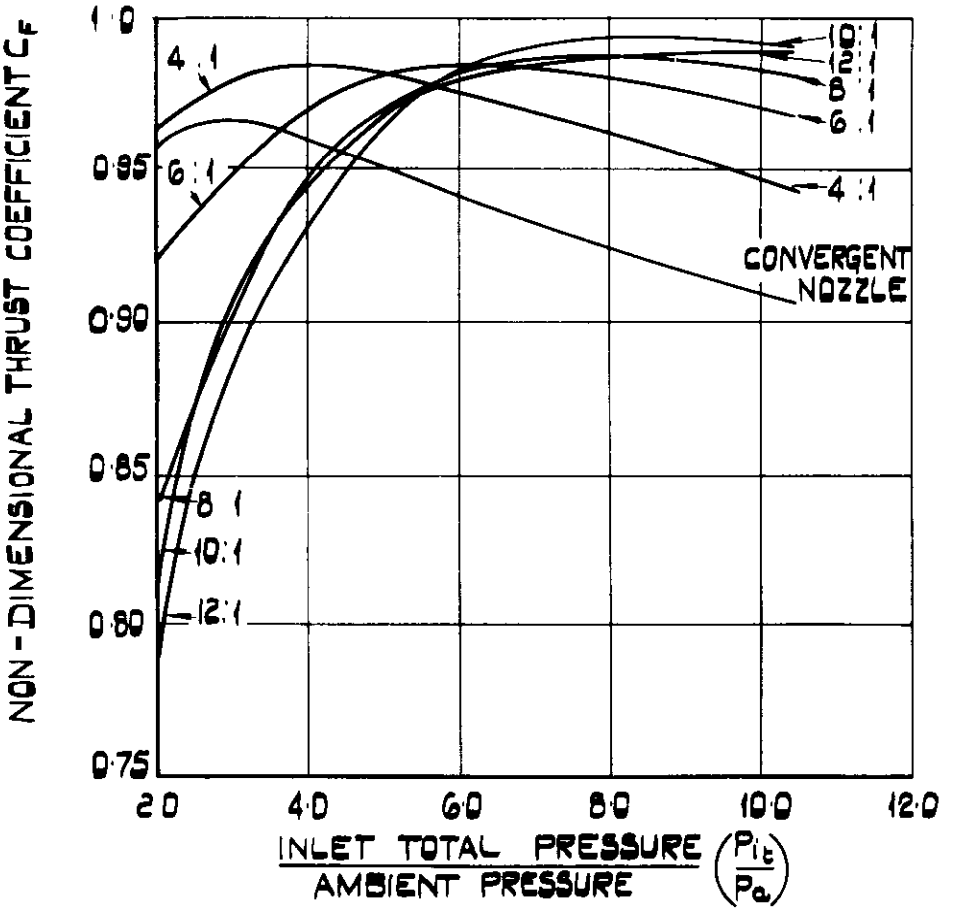

VARIATION OF C_F WITH PRESSURE RATIO FOR GROUP I NOZZLES.

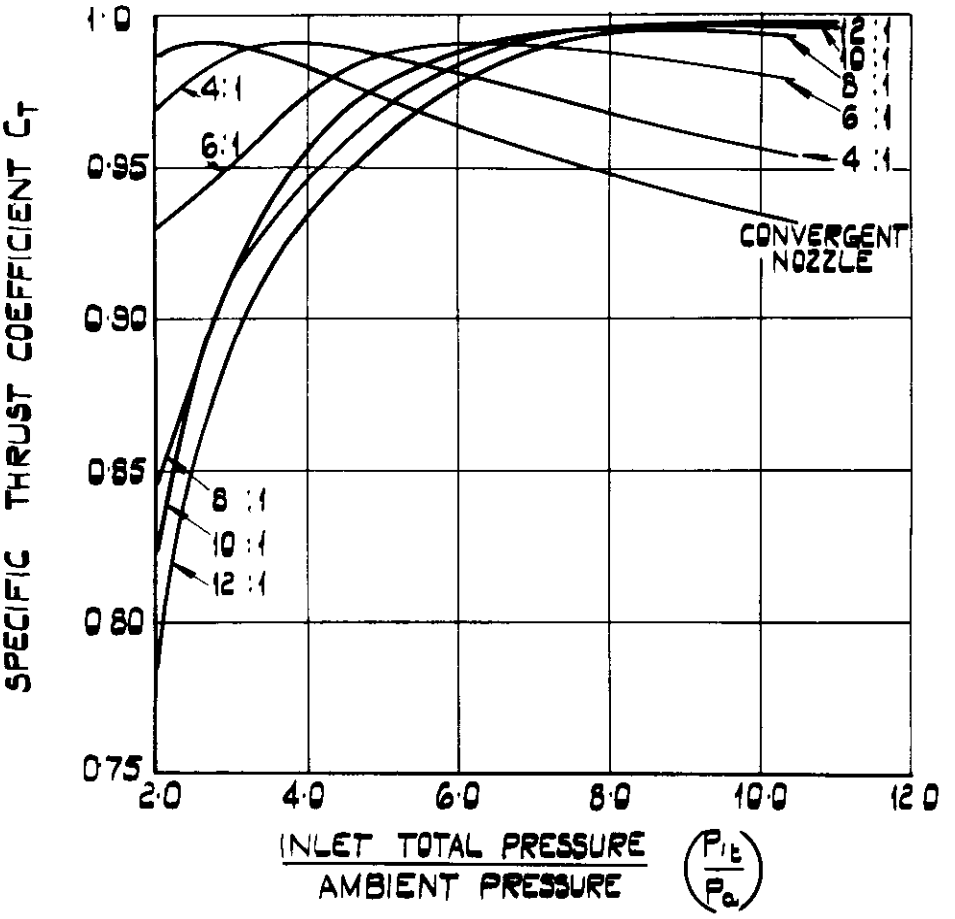

VARIATION OF C_T WITH PRESSURE RATIO FOR GROUP I NOZZLES.

FIG. 9.

SK 5862

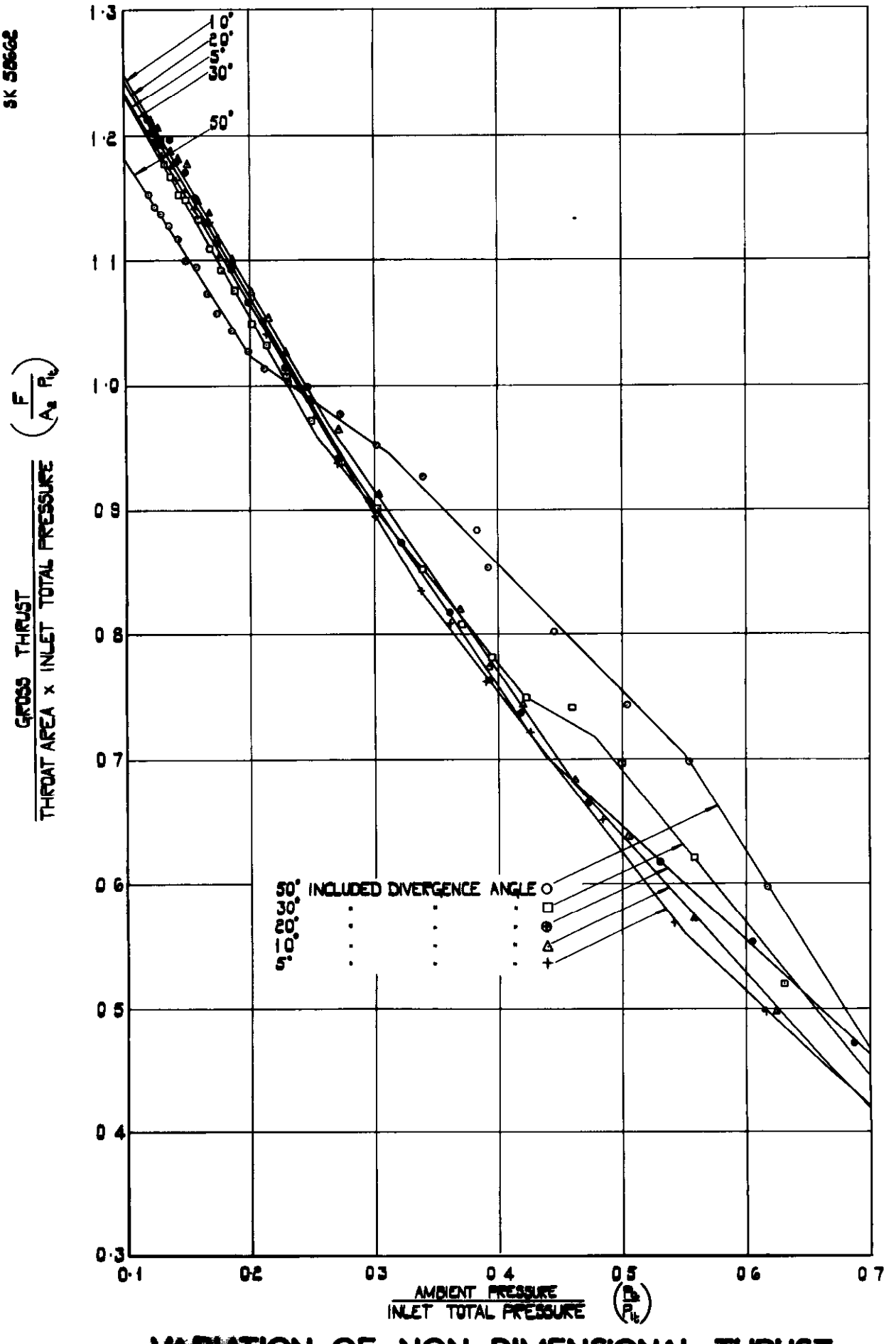

VARIATION OF NON-DIMENSIONAL THRUST WITH PRESSURE RATIO FOR GROUP II NOZZLES.

FIG.10.

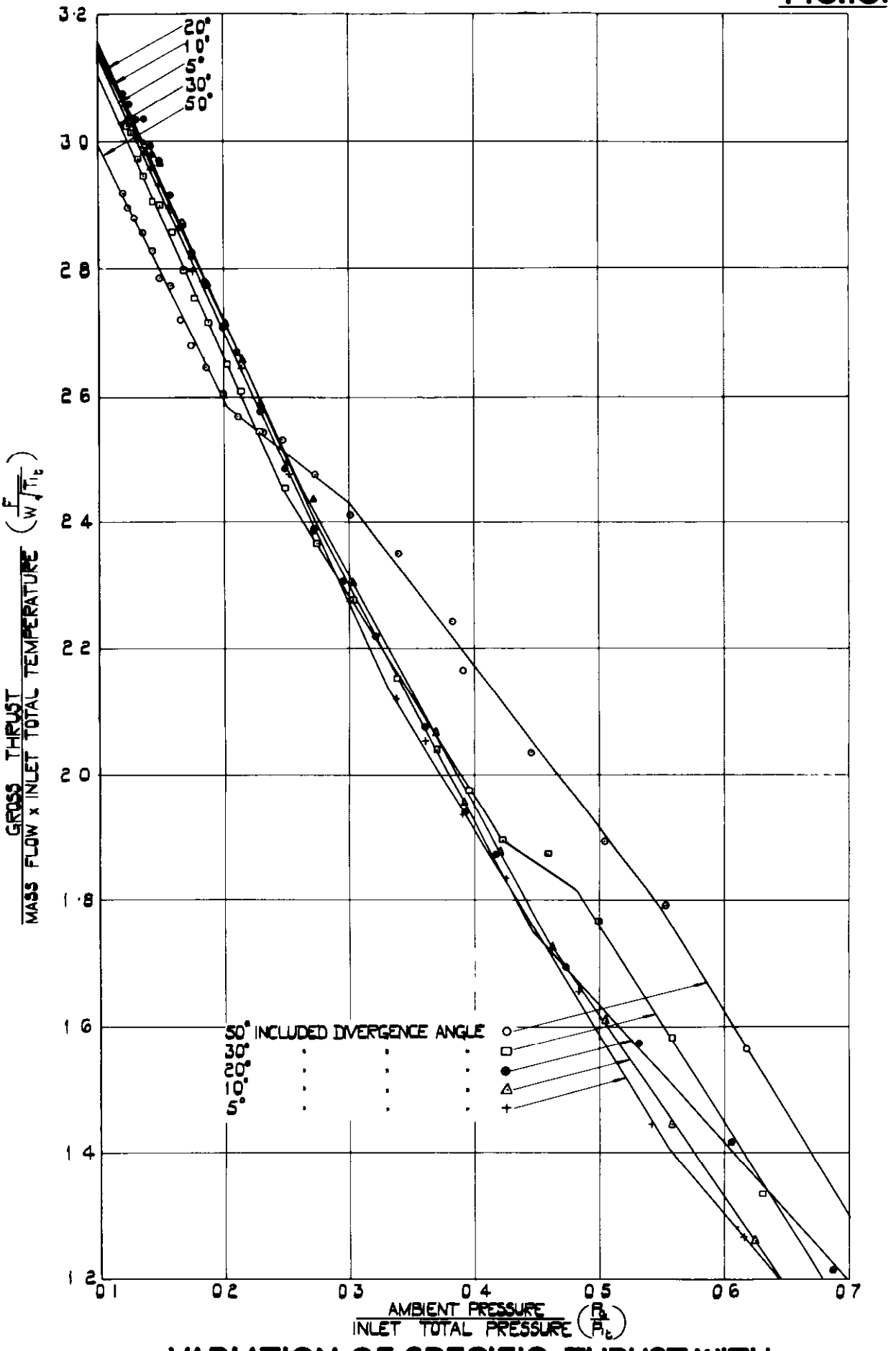

VARIATION OF SPECIFIC THRUST WITH PRESSURE RATIO FOR GROUP II NOZZLES.

SK 60022

FIG.11

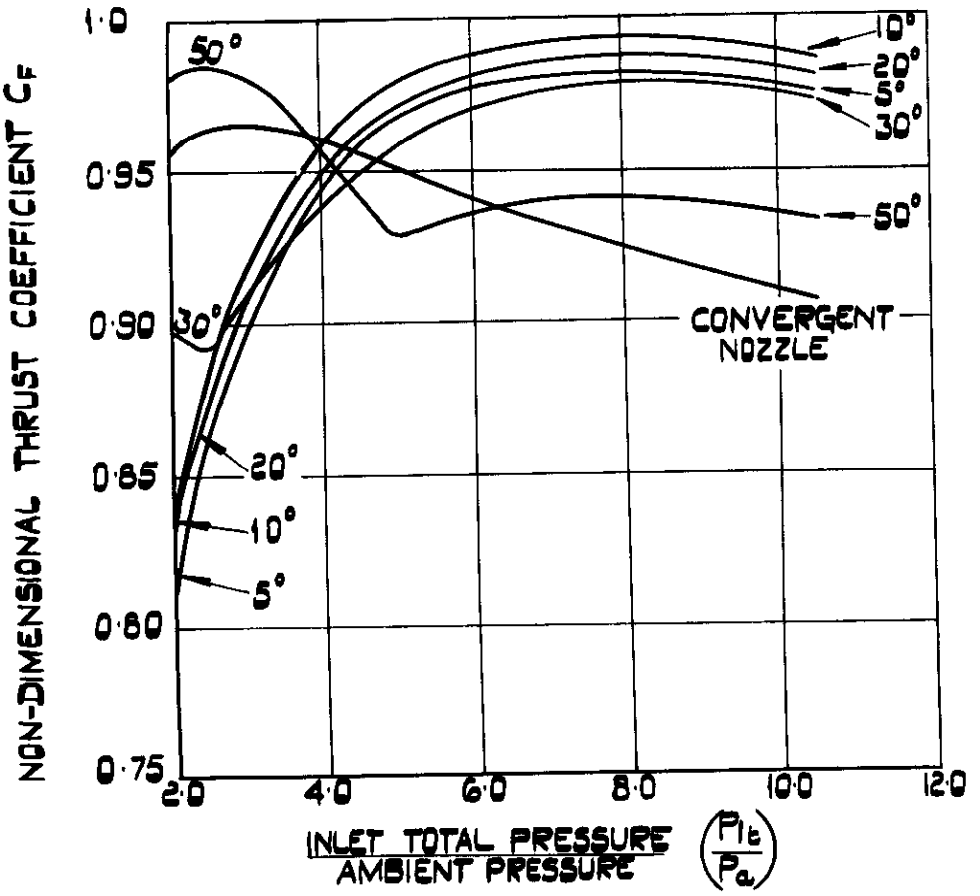

VARIATION OF C_F WITH PRESSURE RATIO FOR GROUP II NOZZLES.

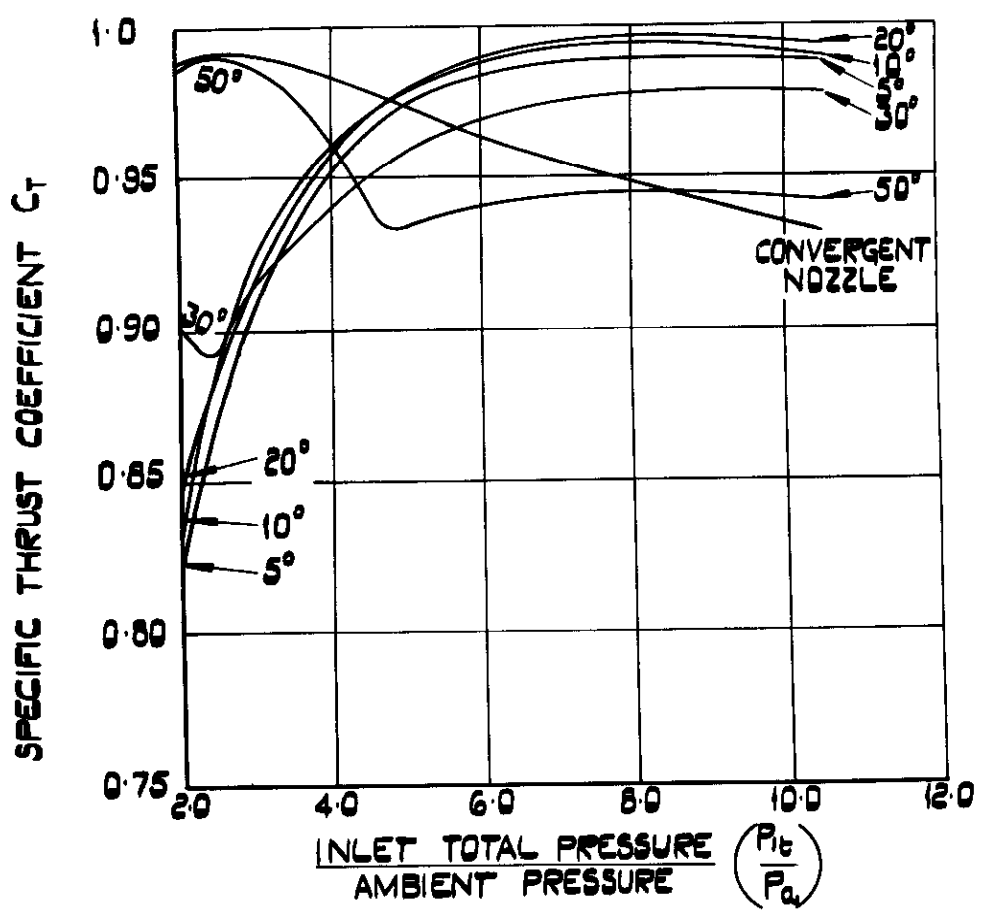

VARIATION OF C_T WITH PRESSURE RATIO FOR GROUP II NOZZLES.

FIG. 12.

SK58663

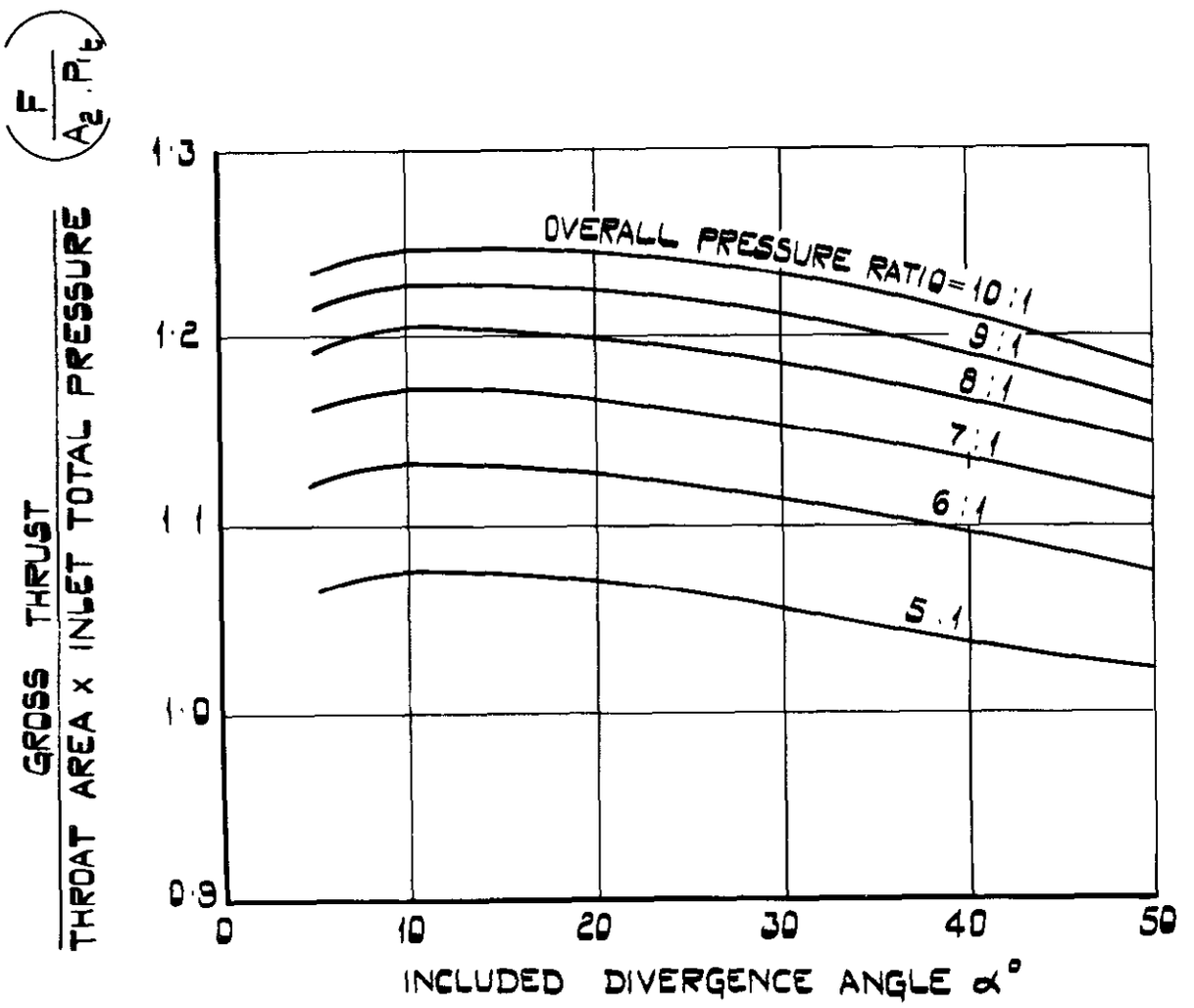

VARIATION OF NON-DIMENSIONAL THRUST WITH INCLUDED DIVERGENCE ANGLE FOR GROUP II NOZZLES.

FIG. 13.

SK 58812

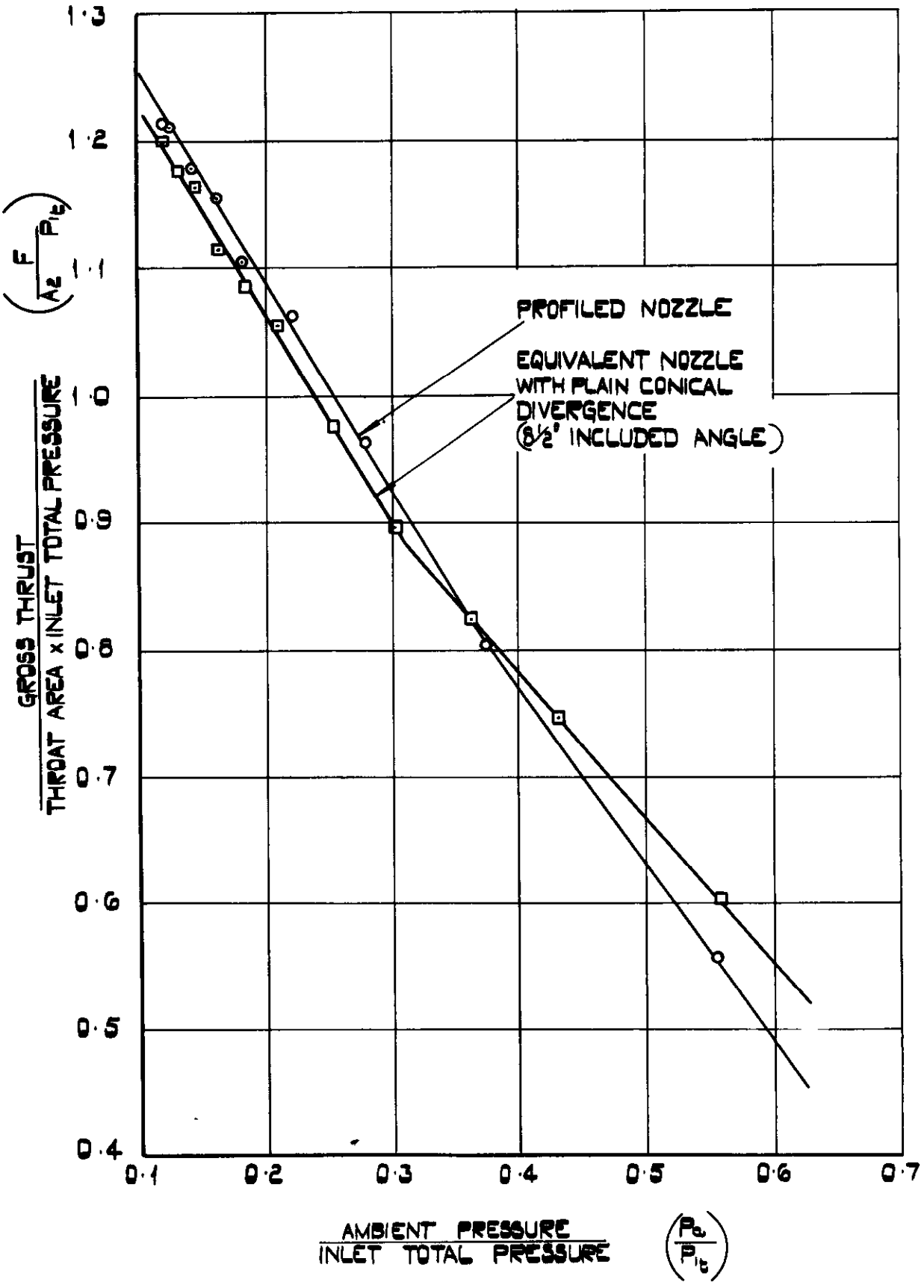

VARIATION OF NON-DIMENSIONAL THRUST WITH PRESSURE RATIO FOR PROFILED NOZZLE AND EQUIVALENT NOZZLE WITH PLAIN CONICAL DIVERGENCE.

FIG. 14.

SK 60166

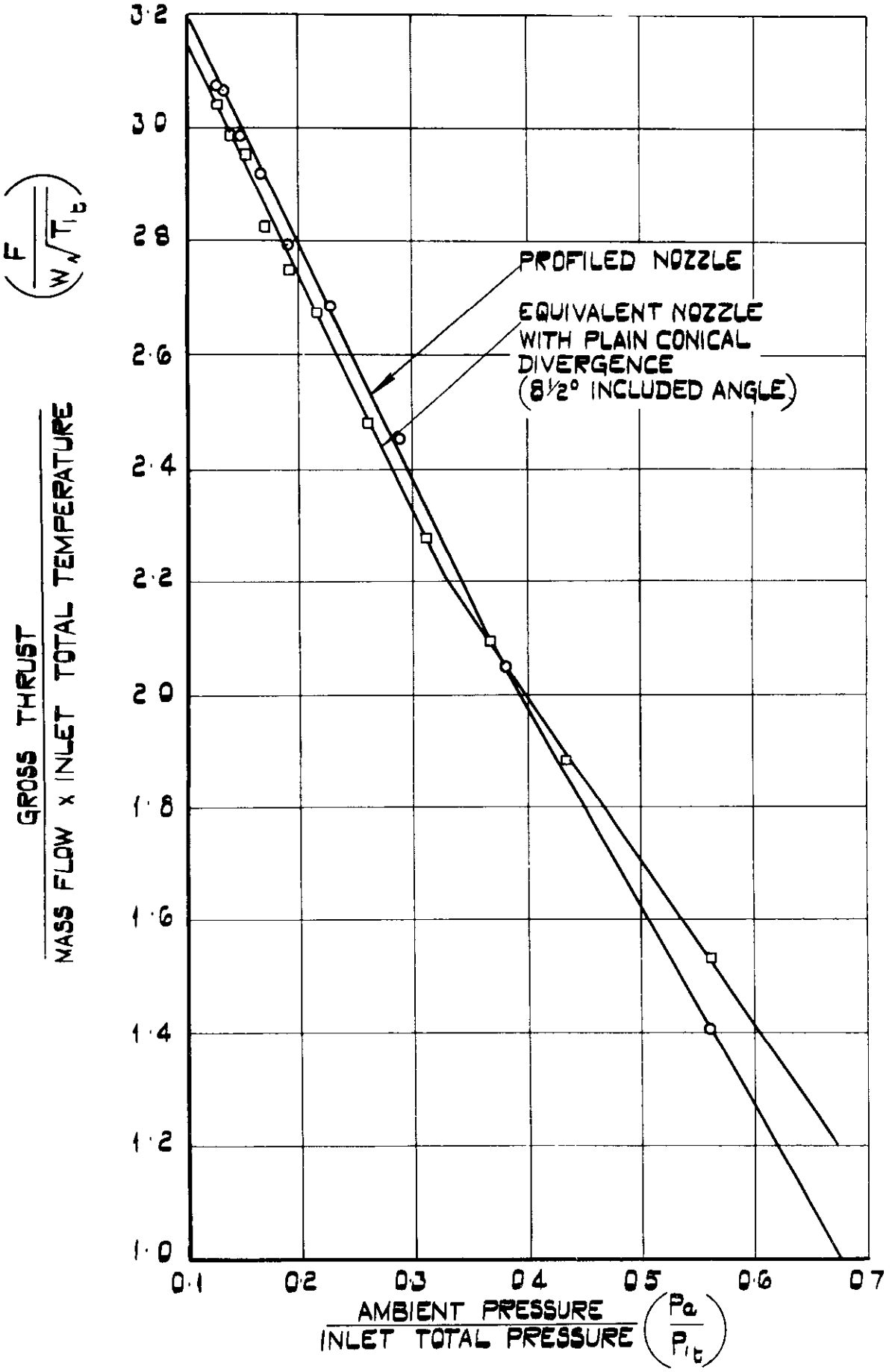

VARIATION OF SPECIFIC THRUST WITH PRESSURE RATIO FOR PROFILED NOZZLE & EQUIVALENT NOZZLE WITH PLAIN CONICAL DIVERGENCE.

SK 58661

FIG. 15

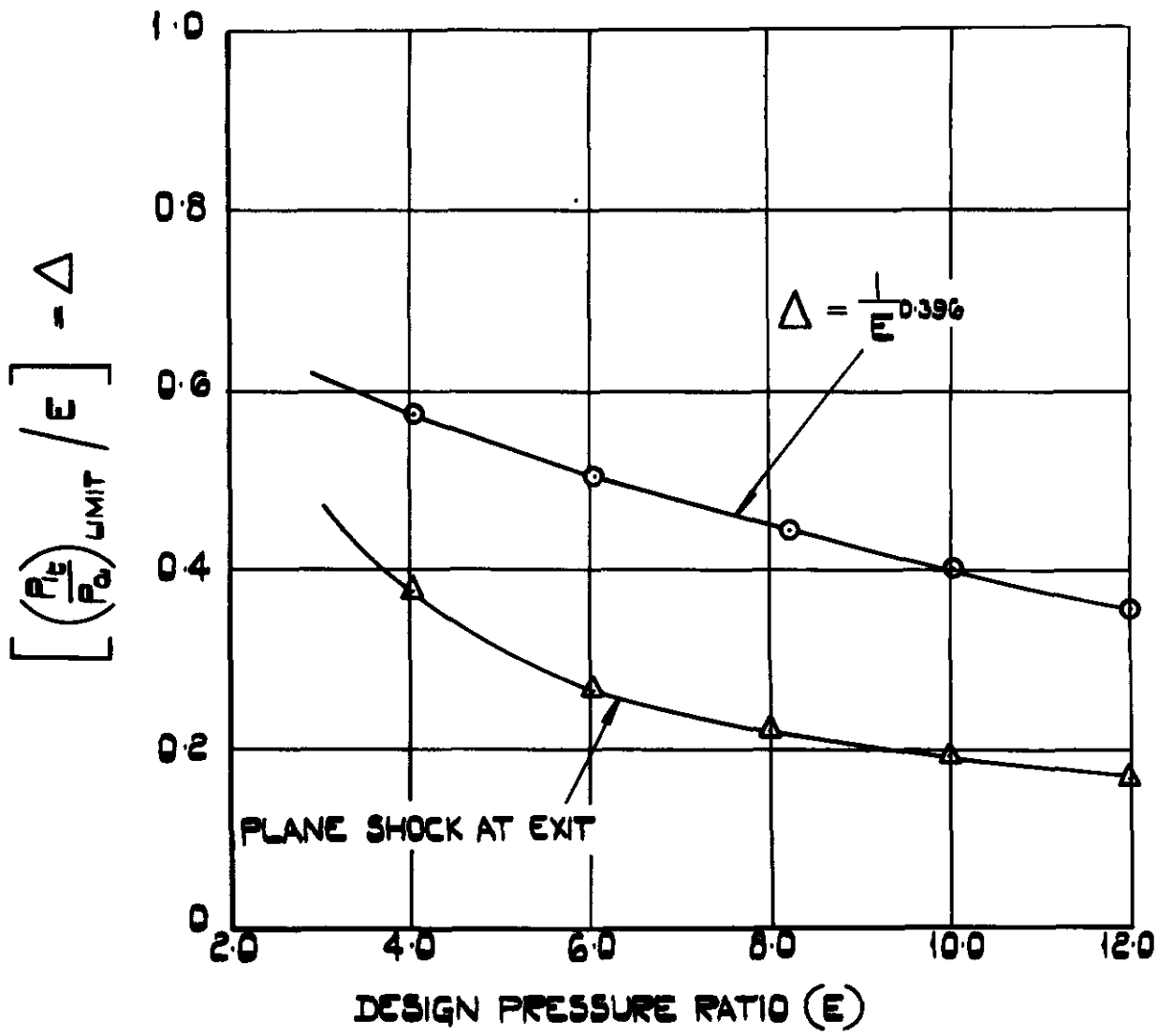

VARIATION OF △ WITH DESIGN PRESSURE RATIO E.

FIG.16.

SK60417

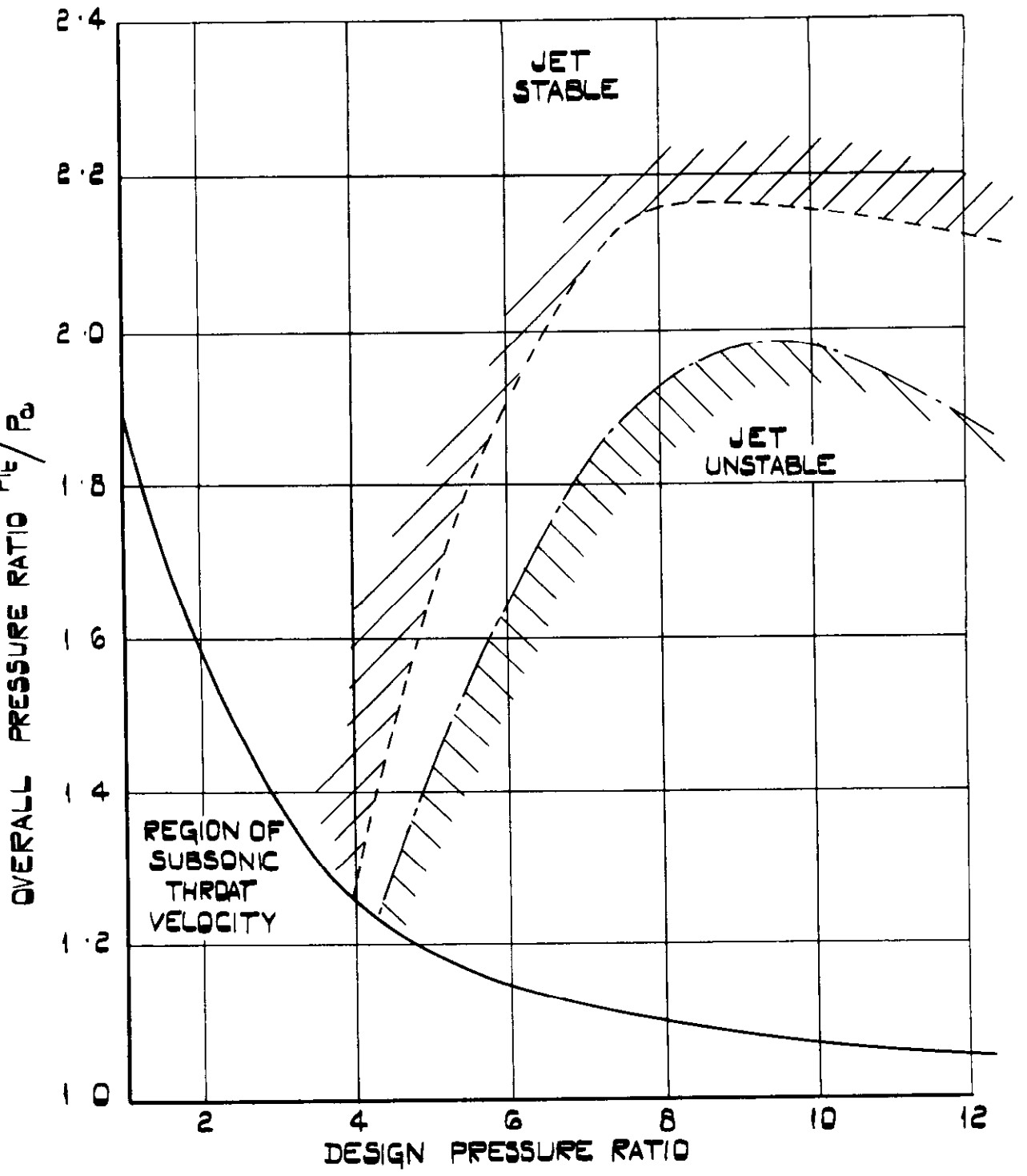

DIAGRAM SHOWING REGIONS OF JET INSTABILITY.

ADDENDUM

The empirical formula for determining the value of Δ, the ratio of the kink point and the design pressure ratios, which is quoted at the bottom of page 8 and shown plotted on Figure 15 has been superseded by later work.

The revised formula, which has been verified experimentally on nozzles having values of design pressure ratio, E, of up to 30, is:-

$$\Delta = \frac{1}{E} + \frac{1}{3}$$

$$\text{that is } \left(\frac{P_{it}}{P_a}\right)_{\text{kink}} = 1 + \frac{1}{3}E$$

The experimental investigation leading up to the derivation of the revised formula is fully described in the following paper:

Measurements of the thrust produced by convergent-divergent nozzles at pressure ratios up to 20.- P. F. Ashwood, G. W. Crosse and Jean E. Goddard. Current Paper No. 326. November, 1956.

C.P. No. 325
(17,833)
A.R.C. Technical Report

Printed and published by
HER MAJESTY'S STATIONERY OFFICE

To be purchased from
York House, Kingsway, London W.C.2
423 Oxford Street, London W.1
13A Castle Street, Edinburgh 2
109 St Mary Street, Cardiff
39 King Street, Manchester 2
Tower Lane, Bristol 1
2 Edmund Street, Birmingham 3
80 Chichester Street, Belfast
or through any bookseller

Printed in Great Britain

S.O. Code No. 23-9010-25
C.P. No. 325